

Influence of Aging Parameters on the Corrosion Resistance of a Biocompatible Ni_{50.6}Ti_{49.4} Shape Memory Alloy

IOANA ARINA GHERGHESCU¹, GABRIELA LILIANA JICMON², COSMIN COTRUT¹, MIHAI BRANZEI¹, ANDREI CONSTANTIN BERBECARU¹, ANDRA MIHAELA PREDESCU¹, SORIN CIUCA^{1*}

¹ Politehnica University of Bucharest, Materials Science and Engineering Faculty, Department of Materials Science and Physical Metallurgy, 313 Splaiul Independenței, 060042, Bucharest, Romania

² Carol I Technical High School, 52 Porumbacu Str., 060366, Bucharest, Romania

The paper shows the results of electrochemical tests made in order to reveal some corrosion resistance features obtained when performing aging heat treatments at different temperatures and holding times on a shape memory Ni_{50.6}Ti_{49.4} alloy. The transformation temperatures of the Ni_{50.6}Ti_{49.4} alloy are already indicating it as a potentially biocompatible one and a final choice must be made after assessing its corrosion resistance as a consequence of the optimum combination choice of the aging temperature and holding time parameters. The best corrosion resistance in artificial saliva after aging heat treatment was found on the sample which was heat treated at 510°C/75 min/ cooled with 5°C/s. The phenomena backing up this conclusion are the raising of the Ti content of the matrix induced by the dynamics of the stable and metastable precipitates formed during the aging, as well as the changes in the stress level associated to the total boundary surfaces between these phases and the matrix.

Key words: NiTi shape memory alloy, corrosion resistance, NiTi precipitates, electrochemical tests

NiTi based shape memory alloys (SMA), such as near-equiatomic NiTi (with a composition of 53 to 57% Ni by weight) present advantages like a high corrosion resistance, a good fatigue resistance and an high biocompatibility, thereby making them one of the most preferred material for the most part of shape memory effect applications being considered today [1].

The shape memory NiTi alloys exhibit a high temperature phase (A or B2, austenite, cubic CsCl - like) and a low temperature phase (M, martensite, monoclinic). Several NiTi alloys sometimes, under certain conditions, may contain the rhombohedral phase known as premartensitic R phase [2]. They are able to be submitted to a shape change at low temperature and remain deformed until they are heated, when they return to their original shape [2].

The most important parameters that characterize a shape memory material are the phase transformations temperatures. These alloys are presenting a hysteretic behavior and there are several relevant temperatures, also called critical points, to be mentioned: the austenite start temperature (A_s), the austenite finish temperature (A_f) during heating, the martensite start temperature (M_s) and the martensite finish temperature (M_f) during cooling. The intermediate phase (R phase) may appear on cooling, exhibiting its own start temperature (R_s) and finish temperature (R_f), before the transformation proceeds to martensite at lower temperatures [3].

When a device made of such a NiTi alloy is deformed at a temperature lower than A_s, it is possible that it transforms to its original form if heated at a temperature higher than A_f. It is worthy to mention that a strain critical value must not be exceeded in order to have the shape memory effect still taking place: shape recovery is possible only up to 8% strain [4].

Another remarkable property of these alloys is their superelasticity, which occurs when NiTi is mechanically deformed at a temperature above its A_f critical point. This

deformation causes a stress induced phase transformation from austenite to martensite. The stress induced martensite is unstable at temperatures above A_f, so that when the stress is removed the material will immediately turn back to the austenite phase and its previous form. This high degree of elasticity, called superelasticity, is the most attractive property of NiTi alloys and the most widely used for. Flexibility, biocompatibility and excellent corrosion resistance are other beneficial properties of these materials.

Still NiTi shape memory alloys also show a number of drawbacks, among them being the manufacturing cost of such an alloy which is quite high.

Due to this unusual macroscopic behaviour, NiTi shape memory alloys applications are numerous: military, medical, safety and robotics applications, from vascular stents to actuators, from vibration protecting devices for buildings to orthodontic wires a.s.o.

NiTi alloys are potentially useful in biomedical applications due to their unique superelasticity behaviour and shape memory effects. However, these alloys are vulnerable to surface corrosion.

Generally speaking, it isn't possible to know in advance the nature of the precipitates formed in such a NiTi alloy subsequent to a heat treatment, no matter its chemical composition. Despite the fact that the equilibrium diagram gives informations on this behavior, according to the chemical composition of a given alloy, structural changes are to be identified by research studies and are often unexpected.

The identification of several precipitates generated by aging heat treatments in a Ni_{50.6}Ti_{49.4} shape memory alloy and of the subsequent changes in the alloy's critical points, the primary characteristic assigning a device applicability, were previously studied and reported [5].

Considering this, the present paper purpose is to investigate the corrosion resistance of the Ni_{50.6}Ti_{49.4} alloy on samples being previously aged at different temperatures and holding times in order to assess its biocompatibility.

* email: sorin.ciuca@upb.ro; Phone: +40729950571

Experimental part

The alloy chosen for the tests was $Ni_{50.6}Ti_{49.4}$. Among richer in nickel NiTi alloys, this is a low one (low nickel NiTi alloys have up to 50.4 % at. Ni and high nickel NiTi alloys have about 51.2% at. Ni).

The $Ni_{50.6}Ti_{49.4}$ alloy samples were obtained as follows:

Titanium plates and nickel bars were used to melt the NiTi alloy. Their purities were:

- Ni 99.7 % (Mn 1100 ppm, Fe 400 ppm, C 400 ppm, Si 300 ppm, Cu 150 ppm, Mg 100 ppm);

- Ti 99.5 % (Fe 1500 ppm, O 1500 ppm, C 200 ppm, N 120 ppm).

The alloy was melted at Metal Products Research Institute of Shanghai. Melting and vacuum casting were performed in a high frequency induction furnace (25 kHz) provided with a calcium oxide crucible, in order to provide the best homogenization of the whole cast [6].

The melting process started at 1700°C in order to prevent the titanium oxidation, further lowering the temperature down to 1450°C. A good ingot surface quality results from casting in water cooled copper moulds. Impurities contamination is insignificant. Before proceeding to plastic deformation, scale is eliminated.

Bars of 5 cm diameter were obtained by forging. The ingot deformation began at 850°C down to 10 mm diameter thin rods. A recrystallization heat treatment at 750°C was performed after forging, followed by several hot extrusions at 800°C, with 15 % reductions between passings. The deformation process ends with a cold wire drawing in such a way that wires of 0.48 mm diameter were obtained.

Following to the hot and cold working stage, the alloy chemical composition was determined by X-ray fluorescence spectroscopy: $Ni_{50.6}Ti_{49.4}$.

In order to exhibit superelasticity or shape memory effect, some heat treatments are usually performed on shape memory alloys. The chosen parameters were the following:

- martensitic quenching, at 750°C/ 25 min / water cooling;
- artificial aging according to table 1. Aging was performed at two different temperatures, two different holding times at the chosen aging temperatures and two cooling rates after reaching and holding at the aging temperature. These parameters are shown in table 1.

Table 1
PARAMETERS CHOSEN FOR THE ARTIFICIAL AGING

No.	Sample no.	Temperature [°C]	Holding time [min]	Cooling rate [°C/ s]
1.	NiTi 1	450	45	5
2.	NiTi 2	510	45	5
3.	NiTi 5	450	45	25
4.	NiTi 6	510	45	25
5.	NiTi 9	450	75	5
6.	NiTi 10	510	75	5
7.	NiTi 13	450	75	25
8.	NiTi 14	510	75	25

Sample no.	Temperature, T [°C]	Cooling rate, v [°C/s]	Holding time, t [min]	M_f [°C]	M_s [°C]	R_f [°C]	R_s [°C]	A_s [°C]	A_f [°C]	Precipitates
NiTi1.	450	5	45	-43.3	-28.7	15	29.2	25.8	36.3	Ni_3Ti_4 , $NiTi_5$
NiTi2.	510	5	45	-38	-30.5	-5.5	13.6	5.7	21.1	Ni_2Ti_3
NiTi9.	450	5	75	-44.9	-31.4	17.4	33	25.5	34.8	$NiTi_2$, Ni_3Ti_4
NiTi10	510	5	75	-36.5	-23.7	-4.1	15.6	13.2	21.8	Ni_2Ti_3 , Ni_3Ti_4

Table 2
AGING PARAMETERS AND TRANSFORMATION TEMPERATURES FOR HEAT TREATED $Ni_{50.6}Ti_{49.4}$ IDENTIFIED BY DSC [5]

The transformation temperatures of these alloys, submitted to aging according to the above - shown conditions, were determined by differential scanning calorimetry [5].

In the first instance one can see that transformation temperatures of this alloy are indicating it as proper to be used in producing biocompatible devices. The highest A_f temperature found in table 2, of 36.3°C, is lower than 37°C and anyway, such a device may be slightly heated in order to recover its initial shape.

Among all samples, NiTi1, NiTi2, NiTi9 and NiTi10 were selected for the corrosion tests, having the same cooling rate after aging. The reason why low cooling rate samples were chosen was to avoid a rise in the internal stress level, potentially leading to a higher martensite content in the material structure. It was aimed to consider samples whose critical points differences are related to the variation of aging parameters (temperature and holding time) consequences, instead of these due to higher cooling rates.

The tests performed on NiTi samples were, as follows:

- electrochemical corrosion tests;
- scanning electron microscopy (SEM) investigations, performed on a FEI QUANTA 450 FEG microscope, equipped with an EDX spectrometra.

Results and discussions

Estimation of corrosion resistance of the $Ni_{50.6}Ti_{49.4}$ alloy

The corrosion behavior of the samples in artificial saliva were studied using electrochemical techniques. Electrochemical measurements were performed at the human body temperature of $37 \pm 0.2^\circ\text{C}$, in a three electrode corrosion cell made of a saturated calomel electrode (SCE) as reference electrode, a platinum counter electrode and the working electrode consisting in the NiTi tested samples. These were previously embedded in resin (acrylic VariDur 10, Buehler) and metallographically prepared (as seen in fig. 3) because any unevenness of the surface influences the corrosion behavior.

The corrosion resistance was determined by the Tafel technique. Tafel plots allow the direct measurement of the corrosion current from which the corrosion rate can be quickly calculated.

This method consists in plotting the linear polarization curves (polarization resistance) involving the following steps:

- measuring the Open Circuit Potential (E_{OC}) for 12 h;
- plotting the potentiodynamic polarization curves between -250 mV (vs OCP) and +250 mV (vs OCP). The scanning rate was of 1 mV/s.

Electrochemical experiments were carried out with a PARSTAT 4000 potentiostat/galvanostat (Princeton Applied Research, USA) associated to a low current box (VersaSTAT LC, Princeton Applied Research, USA). The potentiodynamic curves were acquired with a VersaStudio v.2.43.3 software.

All along the corrosion tests, the corrosion cell together with the low current box were surrounded by a Faraday



Fig.1. The four samples, embedded in acrylic VariDur 10 resin

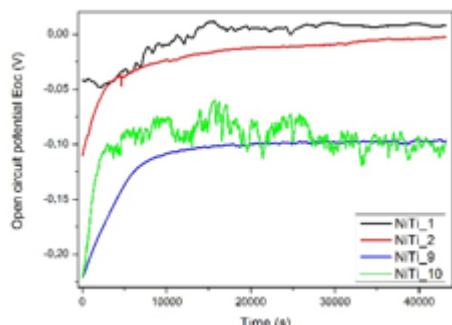


Fig. 2. Evolution of open circuit potential (E_{oc}) of NiTi1, NiTi2, NiTi9, NiTi10 samples in Fusayama Meyer artificial saliva

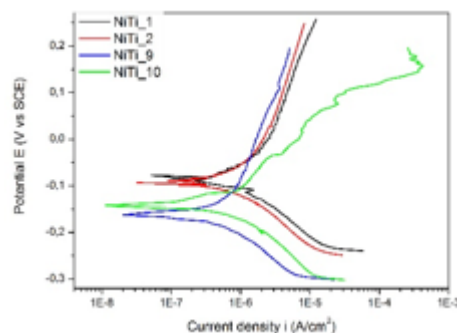


Fig.3. Tafel curves for NiTi1, NiTi2, NiTi9, NiTi10 samples in Fusayama Meyer artificial saliva

Table 3
MAIN PARAMETERS OF THE CORROSION PROCESS

No.	Sample	E_{oc} (V)	E_{corr} (V)	i_{corr} (nA/cm ²)	CR (mm/y)	β_c (mV)	β_a (mV)	R_p (k Ω cm ²)
1	NiTi1	8.357	-81.968	1546	15.604 x10 ⁻³	151.834	378.783	30.48
2	NiTi2	-2.453	-92.704	1643	16.581 x10 ⁻³	168.215	481.717	32.10
3	NiTi9	-96.766	-161.849	785.868	7.929 x10 ⁻³	141.128	436.096	58.98
4	NiTi10	-99.219	-141.032	563.874	5.689 x10 ⁻³	109.715	139.626	47.37

cage in order to exclude electrostatic and electromagnetic influences.

Tests were performed in artificial saliva Fusayama Meyer (composition: 0.4 g/L NaCl, 0.9 g/L KCl, 1 g/L urea, 0.69 g/L NaH₂PO₄, 0.795 g/L CaCl₂ · 2H₂O; pH = 5.2) using a heating bath circulator (CW-05G, Jeio Tech).

The open circuit potential (E_{oc}) variations of the samples tested in artificial saliva Fusayama Meyer were determined, followed by the Tafel curves. For a better understanding, these were superimposed and shown in figures 2, respectively 3.

In order to estimate the corrosion resistance of the tested samples, the following parameters were determined from the Tafel curves: the open circuit potential (E_{oc}), the corrosion potential (E_{corr}), the corrosion current density (i_{corr}), the cathodic curve slope - Tafel constant β_c , the anodic curve slope - Tafel constant β_a .

Their values allowed the calculation of the parameters that describe the tested samples corrosion resistance: corrosion rate (CR) and polarization resistance (R_p).

Table 3 shows the main parameters of the electrochemical corrosion process. The open circuit potential values give proof of the noble character of this alloy.

The formula for calculating the corrosion rate, according to ASTM G102-89 (2004), is the following:

$$CR = K_i \cdot \frac{i_{corr}}{\rho} \cdot EW \quad (1)$$

where:

CR is the corrosion rate (mm/y), K_i is a constant, 3.27 x10⁻³, ρ is the alloy density (g/cm³), i_{corr} is the corrosion current density (nA/cm²) and EW the equivalent weight (g).

Polarization resistance was determined according to ASTM G59-97 (2003) with the formula:

$$R_p = \frac{1}{2.3} \cdot \frac{b_a b_c}{b_a + b_c} \cdot \frac{1}{i_{corr}} \quad (2)$$

where:

β_a is the anodic curve slope, β_c is the cathodic curve slope and i_{corr} the corrosion current density (nA/cm²).

The samples corrosion resistance was estimated according several evaluation criteria.

When considering the value of the open circuit potential (E_{oc}), it is well known that the more electropositive values suggest a better behavior in corrosive media.

Along the electrochemical processes, a decrease of the anodic current shifts the OCP to positive values, aiming a balance of the cathodic current [7]. When immersing a material in an electrolyte, the dissolved oxygen is adsorbed by the NiTi electrode surface and reacts preferentially with titanium, forming a protective film of titanium oxide [8] which inhibits the conductivity of ions at the electrode/electrolyte interface. As a result, the anodic dissolution current decreases as indicated by the rise in the OCP. After a competition between formation and dissolution of the oxide film, a stable anodic dissolution current and thus a steady OCP value is obtained.

The electrochemical measurements showed that most of the samples had open circuit potentials in the negative range excepting the NiTi1 sample that had a positive value of 8.357 mV. One can also notice that samples NiTi9 and NiTi10 had close values, of -96.766 mV and respectively -99.219 mV. According to this criterion the NiTi1 sample has the more electropositive value and consequently a better corrosion resistance.

Furthermore, considering the corrosion potential (E_{corr}), a higher electropositive value denotes a better corrosion behavior in the chosen medium, namely Fusayama Meyer artificial saliva. When examining the resulting values of E_{corr} , one can notice that NiTi1 sample has the higher electropositive value (-81.968 mV) followed by the NiTi2 sample value (-92.704 mV) and then by NiTi10 and NiTi9 samples values. Thus this second criterion reveals one more time that NiTi1 sample has the best corrosion behavior followed by NiTi2 sample that exhibits a very near E_{corr}

value and then by NiTi9 and NiTi10 samples having similar but lower E_{corr} values, as against NiTi1 and NiTi2.

It is well known that a low value of the corrosion current density (i_{corr}) suggests a high corrosion resistance. Hence considering this criterion, the best corrosion behavior is displayed by NiTi10 sample with an i_{corr} value of 563.874 nA. NiTi9 sample has a very close value of i_{corr} of 785.868 nA. NiTi1 and NiTi2 samples exhibit much higher values.

After calculating the corrosion rate (CR) in Fusayama Meyer artificial saliva for all four samples, one can see that the lowest value is obtained for the NiTi10 sample (5.689×10^{-3} mm/y).

Another widely known fact is that a high polarization resistance (R_p) reveals a good corrosion behavior and a low value of this parameter gives evidence of an unsatisfactory behavior in corrosive media. Thus, one can see that NiTi10 and NiTi9 samples show high values of polarization resistance, the highest value being that of the NiTi9 sample, of 58.98 $k\Omega \text{cm}^2$.

Taking into account that i_{corr} , CR and R_p are the topmost criteria when considering a material corrosion resistance, thus one can enframe NiTi9 and NiTi10 samples as having a better corrosion resistance among all the four tested samples, especially NiTi10 sample exhibiting the lowest corrosion current density (i_{corr}), the lowest corrosion rate (CR) and a high polarization resistance (R_p).

Generally speaking, the differences in the microstructural features are responsible for the reported electrochemical parameters. A correlation between them may be commented as follows:

Several precipitates may appear in the structure when submitting to aging a NiTi alloy with more than 50.5 % at.Ni: Ti_3Ni_4 , Ti_2Ni_3 , TiNi_3 . The last one is the only one being a stable phase. But when considering the volume fraction, Ti_3Ni_4 is the most significant precipitate to be found because it enhances mechanical properties due to a very fine precipitation [9].

Many other metastable precipitates are found subsequent to aging. In a $\text{Ni}_{50.6}\text{Ti}_{49.4}$ alloy, several compositions were reported: Ni_3Ti_4 , NiTi_3 , Ni_2Ti_7 , Ni_6Ti_7 [5]. Their presence may be explained by different casting methods, therefore possible microsegregations generating the formation possibility of other metastable precipitates than those reported so far.

It was reported that the improvement of corrosion resistance after annealing is also due to the greater amount of Ni_4Ti_3 precipitates, too small to be observed by SEM and very finely dispersed [10].

It is to be mentioned that improvement of the NiTi corrosion resistance by heat treatment has already been reported. Trepanier et al. [11] investigated the effects of electro-polishing and heat treatments of NiTi stents on their corrosion resistance in Hank's physiological solution at 37°C. These results indicated a significant improvement in the corrosion resistance of NiTi that was attributed to the formation of Ni_4Ti_3 in the matrix and a thin and very uniform Ti-based oxide layer on the surface.

The growth of Ni_4Ti_3 particles by coalescence at 510°C as against their size resulting subsequent to the 450°C aging heat treatment causes a local Ni depletion in the NiTi matrix, thus an increase of its Ti content.

A longer aging holding time of 75 min as compared to 45 min, when aging is performed at the same temperature (NiTi1 vs. NiTi9, NiTi2 vs. NiTi10) has the same effect, of Ni_4Ti_3 particles growing by coalescence.

For comparable heat treatment temperatures and holding times, Bataillard [12] and Frick [9] found that Ni_4Ti_3 precipitates grow by aging treatments up to 550°C (holding

time - 1 h, respectively 1.5 h) and than completely dissolve up to 600°C.

In contact with aqueous media titanium forms on the surface one of its oxides, TiO_2 . The free energy for the formation of nickel oxide is much higher than that of the titanium dioxide. Hence TiO_2 is prone to be formed on the samples surfaces [13], since titanium has a four - fold greater affinity for oxygen than nickel [14].

Thus, by enriching the surface passive film with higher amounts of Ti, they improve the corrosion resistance by the formation of a more protective TiO_2 outer layer [10]. Apart from Ni_4Ti_3 there may be other compositions of precipitates which, by their formation or dissolution, lead to a titanium enrichment of the matrix. For instance, the precipitates reported to be found in NiTi1 and NiTi2 samples (Ni_3Ti_4 , NiTi_3 , Ni_2Ti_3) may contribute, even by partial dissolution, to a raise in the Ti content in the matrix.

Concerning the boundaries-associated stress level, no matter their composition, metastable precipitates have coherent or semi-coherent boundaries with the NiTi matrix. Their higher stress fields as against these of the stable precipitate particles are responsible for inducing the corrosion processes. Usually, structures showing stable precipitates have better corrosion resistance when compared with these containing metastable ones.

A longer aging holding time (75 min vs. 45 min) favours the evolution of metastable precipitates towards stable ones. Such a stable precipitate, Ti_2Ni_3 , was found by scanning electron microscopy in sample NiTi9 [5] and most likely one may assume it is to be found also in sample NiTi10.

Also, when considering only the metastable precipitates coalescence process, a smaller number of larger particles will have a smaller total sum of boundary surfaces, thus a lower boundaries-associated stress level and consequently a better corrosion resistance.

A coalescence phenomenon is generated when rising a heat treatment temperature as well as rising the holding time at a same heat treatment temperature. Both coalescence and metastable-to-stable precipitate evolution are contributing to a better corrosion behaviour. But also dissolution or coalescence of the other rich - titanium precipitates may interfere; this may explain the differences between NiTi9 and NiTi10 polarization resistance values.

Scanning electron microscopy on corroded samples

The SEM micrographs presented below show the morphology of the $\text{Ni}_{50.6}\text{Ti}_{49.4}$ alloy previously submitted to the electrochemical corrosion tests. Taking into account the corrosion resistance results, samples NiTi2 and NiTi10 were examined by scanning electron microscopy in order to find features of the samples surface quality.

Pitting corrosion is a form of extremely localized corrosion that leads to the creation of small holes in the metal. It is a characteristic of metallic materials which are corrosion resistant by a passivation mechanism. When the pitting zones are numerous, the material capacity of

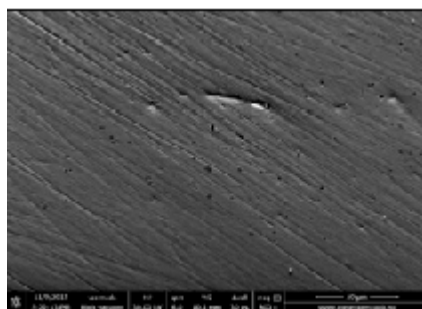


Fig.4. SEM micrograph of NiTi2 sample showing pitting features

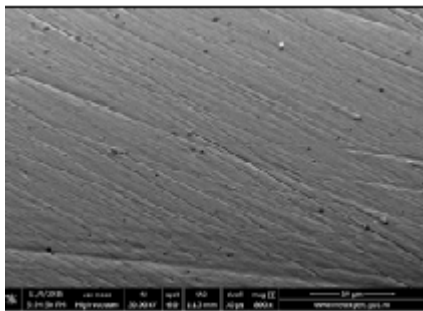


Fig.5. SEM micrograph of NiTi10 sample showing less pitting features than in NiTi2 sample

regenerating the passivated layer is smaller and the resistance corrosion as a whole is lower.

The SEM micrographs of NiTi2 and NiTi10 samples are both showing some pitting holes, but NiTi10 exhibit less pits. This observation is in accordance with the previous electrochemical tests results which stated that sample NiTi10 shows the best electrochemical resistance among all samples.

Conclusions

The best corrosion resistance in artificial saliva after aging treatment was found for sample NiTi10 which was heat treated at 510 °C/ 75 min/ cooled with 5°C/s.

A noticeable amelioration of its corrosion resistance was attributed to the formation of Ni_4Ti_3 in the matrix and to a thin and uniform Ti-based oxide layer on the surface [11], due to the growth of Ni_4Ti_3 particles by coalescence at 510°C as against their size resulting as a consequence of the 450°C aging heat treatment. This causes a local Ni depletion in the NiTi matrix, thus an increase of its Ti content. A longer aging holding time of 75 min as compared to 45 min, when aging is performed at the same temperature (NiTi1 vs. NiTi9, NiTi2 vs. NiTi10) has the same effect, of Ni_4Ti_3 particles growing by coalescence.

Metastable precipitates found in all samples have coherent or semi-coherent boundaries with the NiTi matrix, their stress fields inducing the corrosion processes. Even so, the corrosion resistance is higher in NiTi10 as against the other samples. The stable precipitate Ti_2Ni was found by scanning electron microscopy in sample NiTi9 [5] and most likely one may assume it is to be found also in sample NiTi10, contributing to a rise in the sample corrosion resistance. Also, when considering the metastable

precipitates coalescence process, a smaller number of larger particles will have a smaller total sum of boundary surfaces, thus a lower boundary-associated stress level and consequently a better corrosion resistance. Both coalescence and metastable-to-stable precipitate evolution are contributing to a better corrosion behavior.

Formation or dissolution of all precipitates in sample NiTi10 increase the Ti/Ni ratio of the matrix and thus, by enriching the surface passive film with supplementary amounts of Ti, they improve the corrosion resistance by the formation of a more protective TiO_2 layer.

Considering the greater affinity to oxygen of Ti as against Ni, a uniform Ti based oxide layer is explaining, together with changes in stable and metastable precipitates, the material electrochemical stability.

References

1. GUENIN, G., *Alliages à mémoire de forme*, **N1**, nr. M530, Techniques de l'ingénieur, Lyon, 1986, p. 1.
2. LIU, Y., KIM J.I., MIYAZAKI S., *Philos. Mag.*, **84**, no. 20, 2004, p. 2083.
3. SHAW, J.A., CHURCHILL, C.B., IADICOLA, M.A., *Exp. Tech.*, **32**, no. 5, 2008, p. 55.
4. HODGSON, D.E., WU, M.H., BIERMANN, R.J., *ASM Handbook*, Vol.2, Nonferrous Alloys and Special-Purpose Materials, 1990, p.897.
5. GHERGHESCU, I.A., TARCOLEA, M., JICMON, G.L., PURCA^a, C.V., *Rev. Chim.(Bucharest)*, **64**, no. 4, 2013, p. 407.
6. BUJOREANU, L.Gh., *Materiale inteligente*, Junimea, Iasi, 2002, p. 23.
7. CHENG, X.L., ROSCOE, S.G., *Biomaterials*, **26**, 2005, p. 7350.
8. FIGUEIRA, N., SILVA, T.M., CARMEZIM, M.J., FERNANDES, J.C.S., *Electrochimica Acta*, **54**, Issue 3, 2009, p. 921
9. FRICK, C.P., ORTEGA, A.M., TYBER, J., MAKSSOUND, A.EL.M., MAIER, H.J., LIU, Y., GALL, K., *Mat.Sci.Eng. A-Struct*, **405**, Issue 1-2, 2005, p. 34.
10. MAN, H.C., CUI, Z.D., YUE, T.M., *Scr. Mater.*, **45**, 2001, p.1447.
11. TREPANIER, C., TABRIZIAN, M., YAHIA, L'H., BILODEAU, L., PIRON, D.L., *J.Biomed.Mater.Res.*, **43**, Issue 4, 1998, p. 433.
12. BATAILLARD, L., BIDAUX, J.E., GOTTHARDT, R., *Philos. Mag.*, **78**, no. 2, 1998, p. 327.
13. MICHIARDI, A., APARICIO, C., PLANELL, J.A., GIL, F.J., *J. Biomed. Mater. Res. Part B: Appl. Biomater.*, **77B**, Issue 2, 2006, p. 249.
14. CHU, C.L., HU, T., WU, S.L., DONG, Y.S., YIN, L.H., PU, Y.P., LIN, P.H., CHUNG, C.Y., YEUNG, K.W.K., CHU, P.K., *Acta Biomater.*, **3**, Issue 5, 2007, p. 795

Manuscript received: 21.01.2016